Surface Review and Letters, Vol. 24, No. 4 (2017) 1750055 (13 pages)

DOI: 10.1142/S0218625X1750055X

World Scientific
www.worldscientific.com

# EFFECT OF INHIBITOR AGENTS ADDITION ON CORROSION RESISTANCE PERFORMANCE OF TITANIA SOL–GEL COATINGS APPLIED ON 304 STAINLESS STEEL

ALI SHANAGHI*,‡, PAUL K. CHU†,§ and HADI MORADI*
*Materials Engineering Department, Faculty of Engineering,
Malayer University, Malayer, Iran

†Department of Physics & Materials Science, City University of Hong Kong,
Tat Chee Avenue, Kowloon, Hong Kong, P. R. China
‡alishanaghi@gmail.com; a.shanaghi@malayeru.ac.ir
§paul.chu@cityu.edu.hk

Received 11 April 2016
Revised 7 September 2016
Accepted 7 September 2016
Published 6 October 2016

Hybrid organic–inorganic coatings are deposited on 304 stainless steel substrates by the sol–gel technique to improve the corrosion resistance. A titania-based nanostructured hybrid sol–gel coating is impregnated with three different microencapsulated healing agents (inhibitors) including cerium, *Benzotriazole* (BTA), and 8-*Hydroxyquinoline* (8H). Field-emission scanning electron microscopy (FE-SEM) and electrochemical impedance spectroscopy (EIS) are performed to investigate the barrier performance properties. The optimum conditions to achieve corrosion protective coatings for 304 stainless steel were determined. The Nyquist plots demonstrate that the activation time of the coating containing 8H as an organic healing agent shows improved behavior when compared to other coatings including cerium and BTA. Cerium as an inorganic healing agent is second and BTA is third and minimum. An increase in the impedance parameters such as resistance and capacitance as a function of immersion time is achieved in a 3.5 wt.% NaCl solution by using healing agents such as BTA. Actually, over the course of immersion, the barrier performance behavior of the coatings changes and reduction of the impedance observed from the coatings containing Ce and 8H discloses deterioration of the protection system after immersion for 96 h of immersion in the 3.5% NaCl solution. However, after 96 h of immersion time, the concentration of chloride ions is high and causes increase in defects, micro cracks, hole on the surface of hybrid titania nanostructured coating containing Ce and 8H by destruction of coating, and also hybrid titania nanostructured coating containing BTA; BTA is released from coating to improve the resistance of passive film, which is created on the surface.

*Keywords*: Hybrid ceramic base coating; nanostructure; titania; inhibitor; sol–gel; 304 stainless steel; corrosion resistance.

## 1. Introduction

Hexavalent chromate is widely used in industrial application to produce protective coatings.[1,2] Owing to the toxicity of chromium (VI), there has been increasing focus on the environmental and health problems caused by chromium (VI) and new corrosion-resistant coating systems are being explored.[3–9] Coatings can deteriorate due to a number

‡Corresponding author.

of reasons such as the use of incorrect coatings, defective coatings, corrosive environments and exposure to unexpected outside environments.[4] Inspired by a variety of natural materials, the study in production of self-healing materials focuses on the preparation of multifunctional materials that are able to recover their basic properties including mechanical strength, conductivity, fracture toughness, and corrosion resistance, after damage has occurred.[5] Passive protective coatings are among the most widespread approaches for corrosion protection of metallic substrates. These coatings limit corrosion initiation by restricted ingress of water and corrosive species to the metal coating interface.[6]

It is mentioned that most of the research work in self-healing area is focused on the polymers and polymer composites as these materials are used excessively in everyday and industrial applications, but the thickness of coating is more than 50 $\mu$m.[5] However, self-healing ceramic-based materials with imperative self-healing effects are expected to result in the incorporation of a number of merits as well as in resolving the traditional problems of ceramics and their respective composite materials, such as crack, porosity and so on. In this respect, self-healing coatings may improve the corrosion protection of metals. Self-healing coatings are engineered to provide superior resistance to corrosion, especially when the coating is breached or stressed (mechanically or chemically).[10] They also offer continuous protection even if the surface is partially damaged. These beneficial properties can be achieved by impregnating corrosion inhibitors into the coating system because they can provide local protection in places where the coating is damaged.[11] However, the main purpose of self-healing ceramic-based coating, in order to make the case when small defects accrue by cavitation or corrosion mechanism, releasing the inhibitor and flow to defects caused to produce suitable products of corrosion and prevent the growth of holes or further corrosion. Since this process is done without human intervention, this coating and its mechanism are considered as self-healing coatings.

There are several techniques to deposit self-healing coatings, for instance, physical vapor deposition (PVD), electrochemical deposition, and the sol–gel method. Among them, the sol–gel technique is effective in producing adherent and chemically inert oxide or hybrid films at a low temperature ($< 200^{\circ}$C) which is required for steel substrates.[12–14] In addition, sol–gel thin films have been prepared to contain either inorganic (e.g. cerium) or organic inhibitors (e.g. *Benzotriazole* (BTA)).[15–17]

Austenitic stainless steels are of interest as structural materials in the chemical and petroleum industry. Austenitic stainless steels suffering from corrosion failure in localized areas increase the production and replacement costs.[18,19] Cr (VI) compounds are among the most common substances used for corrosion protection, but these compounds are highly toxic, and an intense effort is being undertaken to replace them. The sol–gel method is a new alternative process to develop coatings in order to improve the corrosion behavior of the whole systems, such as titania nanostructured coating prepared using the sol–gel method and deposited on AISI 304 substrates.[20–22] These coatings extend the lifetime of the substrate, and when an organic or inorganic functionality is attached to the titanium atom, the thickness of crack-free coatings can be increased. The preparation of coatings by dipping substrates in sol–gel solutions is an established method to produce homogeneous coatings with uniform thickness.[20–23] In this study, hybrid organic–inorganic self-healing coatings are deposited on austenite stainless steel by the sol–gel technique and the effects on the impregnated inhibitors on the corrosion resistance are evaluated by electrochemical techniques.

Passive protective coatings are among the most widespread approaches for corrosion protection of metallic substrates. Such coatings restrict ingress of water and corrosive species to the metal coating interface, limiting corrosion initiation.[1,2] Due to the electrochemical nature of the corrosion processes, electrochemical characterization techniques are well-suited for evaluation of the coating's protective performance.

## 2. Experimental Details

304 austenite stainless steel samples were used as the substrate materials. After polishing to a surface roughness of approximately $R_a = 2\,\mu$m using $Al_2O_3$ slurry, the samples were cleaned with acetone and then ultrasonically cleaned in ethanol. $TiO_2$ as an interlayer and sol–gel coating was deposited on the substrates. The $TiO_2$ sol was prepared from tetra-*n*-butyl titanate (TBT), ethanol, ethyl acetoacetate (EAcAc), poly ethylene glycol (PEG), and distilled water at room temperature (first solution according

to Fig. 1(a)). The solution was synthesized by hydrolysis of the 3-glycidoxypropyltrimethoxysilane (GPTMS) solution in absolute ethanol. The $TiO_2$ sol–gel solution without PEG was added dropwise to the GPTMS-based solution to form the hybrid sol–gel solution. Inorganic corrosion inhibitors, $Ce(NO_3)_3$, and organic inhibitors, BTA and 8-hydroxyquinoline (8H), were added to the hybrid sol–gel solution (second solution according to Fig. 1(b)). After aging the solution for 10 h, the cleaned samples were coated by a dip coater rig at a dip coating rate of 0.5 mm/s in the $TiO_2$ solution (first solution). The deposited titania film was aged at 100°C and calcinated at 180°C for 1 h in air to remove organic compounds. The samples were dried and heated to 400°C in a tube furnace. Afterwards, the samples were immersed for 1 min in the $Ce(NO_3)_3$ (5 g/L of ethanol), BTA (20 g/L of ethanol), or 8H (20 g/L of ethanol) solution and dried for 1 h at 80°C. Finally, the self-healing coatings, which had been incorporated with three different self-healing agents (second solution, Fig. 1(b)), were applied by the dip-coating method and cured at 110°C for 1 h in air for cross-linking and gelation of the sol–gel coating and solvent evaporation. It is mentioned that this process was repeated for five times to obtain appropriate thickness (more than 3 $\mu$m) and samples were dried between each deposition for 1 h at 80°C.

The crystalline structure of the self-healing coating was determined by grazing incidence X-ray diffraction (GIXRD) (Philips PW-1730 diffractometer) in the continuous scanning mode using $CuK_\alpha$ radiation ($\lambda = 0.154056$ nm). The surface morphology, film uniformity, and homogeneity were studied by field-emission scanning electron microscopy (FE-SEM, Philips) and atomic force microscopy (AFM), and the thickness of coating was measured by using ellipsometry. The corrosion properties of coatings were investigated by salt spray research, which was done according to ASTM B117 standard in fog of

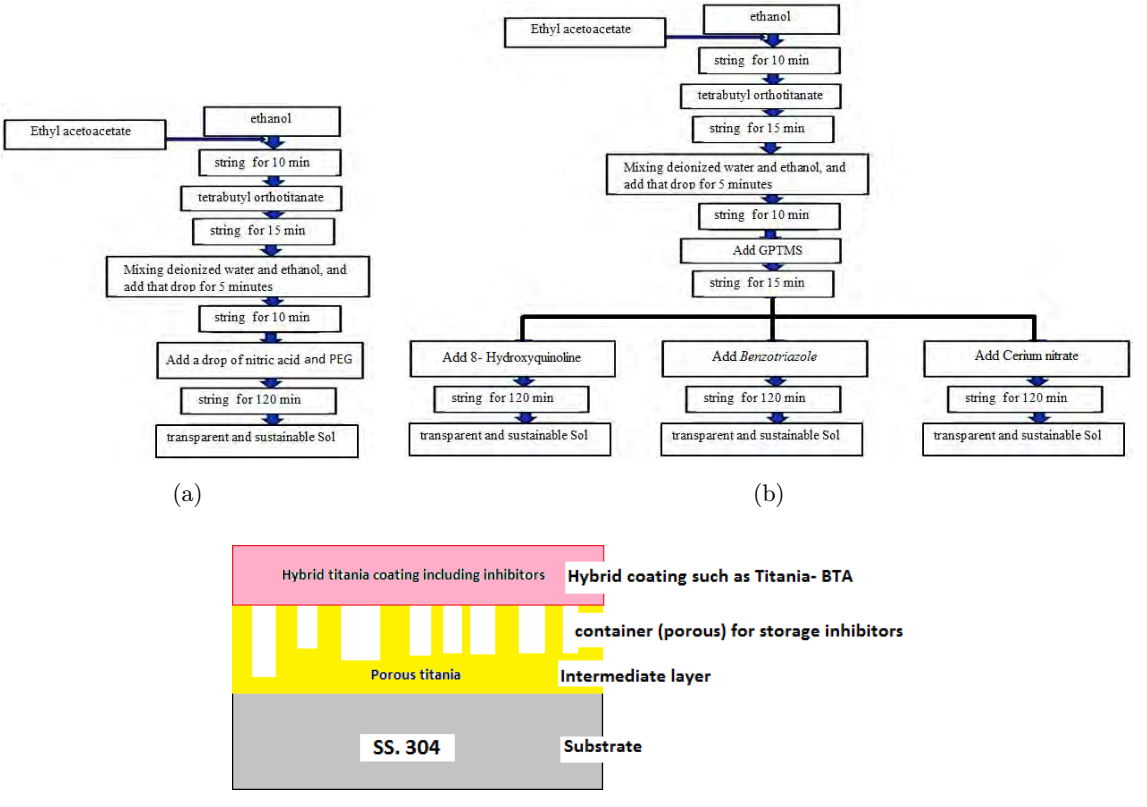


Fig. 1. Schematic preparation diagram for sol–gel derived (a) titania solution for intermediate layer and (b) hybrid sol–gel solution with inhibitors such as BTA, Cerium and 8H and also (c) schematic of applied coating on SS.304.

3.5 wt.% NaCl solutions at the temperature of 37°C up to 500 h, and the coatings were cross scratched following ASTM D1653. These samples were irregularly evaluated at 24 h interval and samples were taken out when the corrosion occurred. After the test and appearance of the red rust, the corrosion products were removed, and the samples rinsed with acetone and dried, then the weight loss of samples was determined. Also, the corrosion properties of the coatings were evaluated by electrochemical impedance spectroscopy (EIS) in a 3% NaCl solution in air at room temperature for up to 96 h. EIS was performed between 0.01 Hz and 100 kHz on a frequency response analyzer (Electrochemical analyzer instrument: CompactStat Ivium Soft 1.805 Release IVIUM Technologies Netherlands).

## 3. Results and Discussion

In the sol–gel technique, careful control of the processing steps such as hydrolysis and condensation of metallic alkoxides are needed to obtain the desired molecular mixture, especially inorganic nanoparticles in an organic matrix.

Figure 2 shows the XRD spectra of the porous coating and coated samples containing the three different self-healing agents. The coatings have an amorphous structure. The XRD pattern of the $TiO_2$ intermediate layer deposited on the 304 stainless steel substrate exhibits diffraction peaks corresponding to $TiO_2$ phases such as rutile as well as anatase and it is in a good agreement with the reported data.[11] A high-temperature thermal treatment considerably changes the structure and composition of the self-healing coating, especially the nature of the healing agents.[11] Therefore, the samples coated with the $TiO_2$ intermediate layer and loaded with the inhibitors are thermally treated at 110°C only.

Figure 3 depicts the FE-SEM micrograph of the porous titanium oxide nanoparticle coating and deposited silica–titanium nanocomposite coating containing the three different self-healing agents. A porous structure is observed from the $TiO_2$ intermediate layer. The nanoporous $TiO_2$ structure enhances

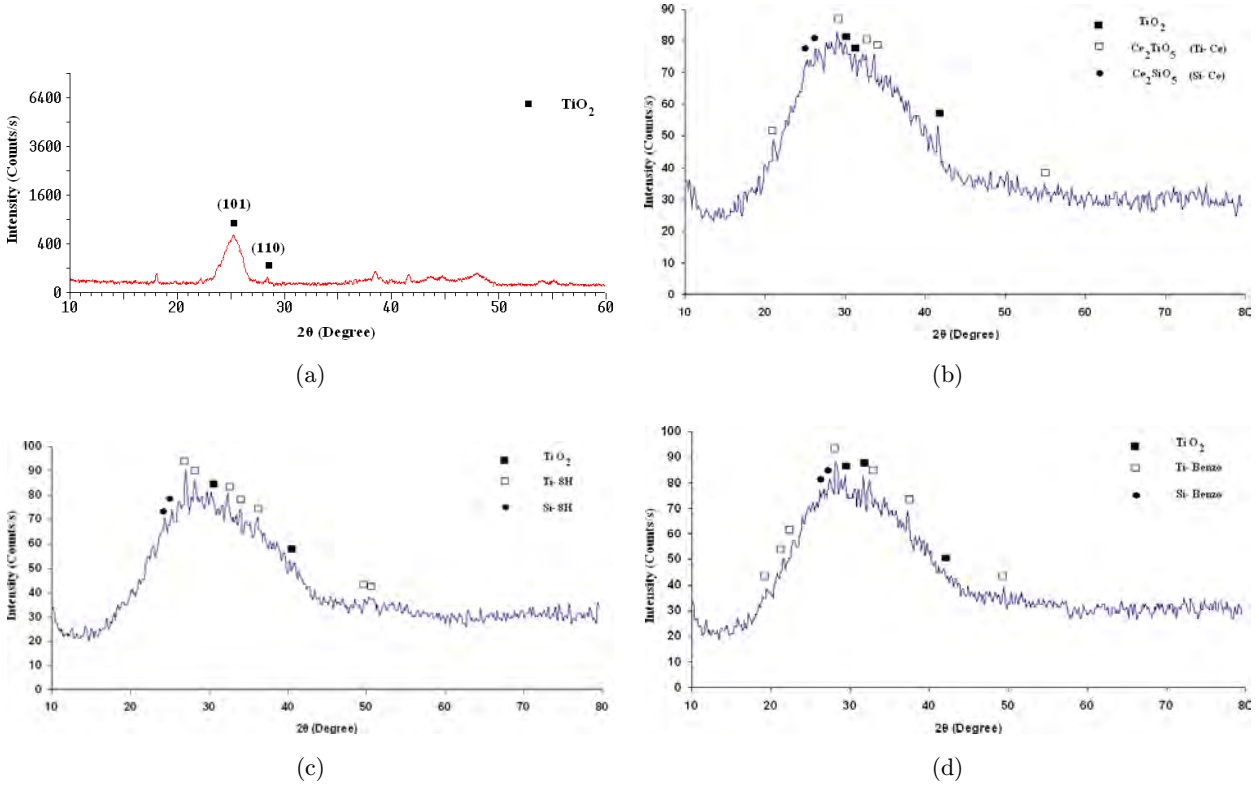


Fig. 2. XRD spectra of (a) titania porous coating and titania coatings containing three different self-healing agents: (b) Ce, (c) 8H and (d) BTA.

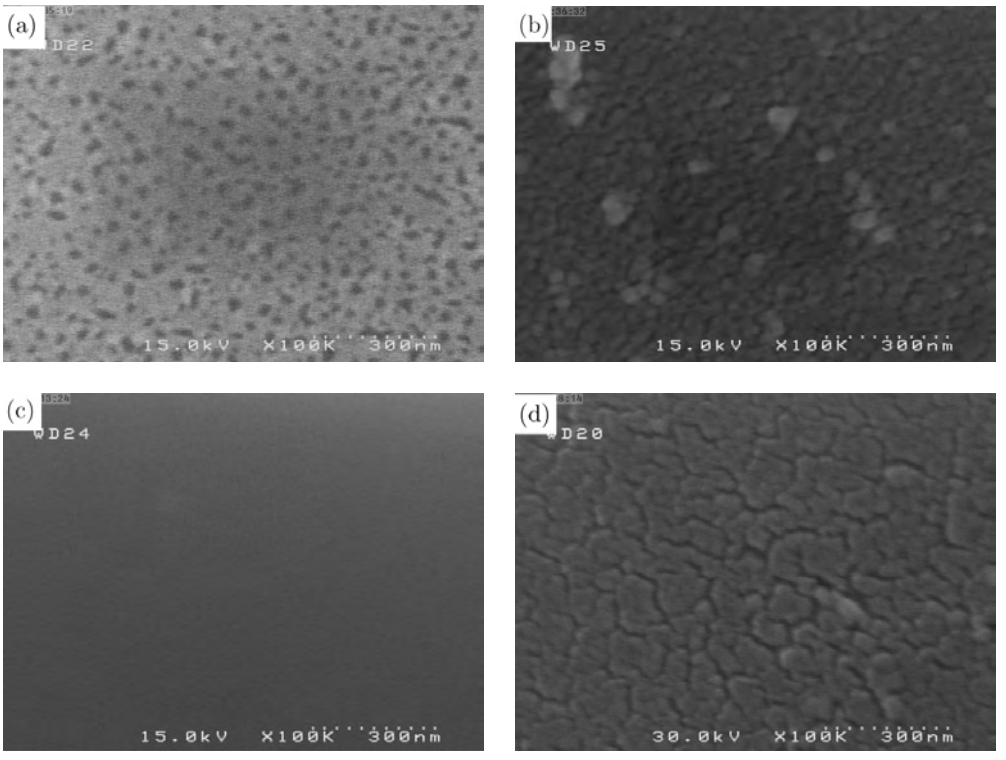


Fig. 3. FE-SEM micrographs of (a) porous titanium oxide nanoparticle coating and self-healing coatings containing three different self-healing agents: (b) Ce, (c) 8H and (d) BTA.

the homogeneous distribution of the healing agents in the coating and also increases the $TiO_2$ porosity desirably from the viewpoint of the loading capacity. The synthesized self-healing coatings are uniform and homogeneous, and the addition of different inhibitors does not significantly change the thickness of coating which is about 3 $\mu$m.

AFM results and thickness of titania nanostructured coating with three different inhibitors such as BTA, Cerium and 8H are summarized in Table 1, and also based on $R_q$ parameter, the reduced roughness was calculated according to Eq. (1).

$$\text{Reduced roughness (\%)} = \frac{|R_{q\text{Titania}-\text{inhibitor}} - R_{q\text{Titania nanostructured coating}}|}{R_{q\text{Titania nanostructured coating}}} \times 100. \quad (1)$$

$R_a$, $R_q$ and $R_{\max}$ are average roughness surface or vertical deviations from the ideal level, the root mean square (rms) average roughness of a surface and the highest peak or maximum roughness, respectively.

Table 1. AFM results and thickness of titania nanostructured coating with three different inhibitors such as BTA, cerium and 8H.

| Coating | $R_a$ (nm) | $R_q$ (nm) | $R_{\max}$ (nm) | Thickness of coating for one dip-coating (nm) | Final thickness of coating ($\mu$m) | Reduced roughness (%) |
|---|---|---|---|---|---|---|
| Titania nanostructured coating | 21 | 25.1 | 39 | 430 | 2.150 | — |
| Titania-cerium | 0.25 | 0.29 | 1.38 | 910 | 4.550 | 98.8 |
| Titania-8H | 0.07 | 0.08 | 0.42 | 810 | 4.050 | 99.7 |
| Titania-BTA | 0.21 | 0.25 | 0.93 | 830 | 4.150 | 99 |

According to the data in Table 1, the surface roughness of the coating containing 8H is lower than other samples. Actually, the mismatch in the coefficients of thermal expansion influences the S.S 304-ceramics coating bonding. During the heat treatment of the titania composite nanostructured coating, generation of stress between the metal substrate and ceramic coating as a result of a difference in thermal contraction and expansion decreases the bonding strength of the coating. Furthermore, mechanical stress is accumulated during subsequent heat treatment of the coating.[5,6] The quantity of surface roughness can predict a real object interaction with its environment. The high value of the roughness, prepares the surface layer to create cracks and destruction layers. Although the addition of 8H leads to a significant reduction in $R_a$, $R_q$ and $R_{\max}$, it is noteworthy that afterwards addition of BTA and cerium increases $R_a$, $R_q$ and $R_{\max}$ and the heterogeneous property of surface.

In fact, releasing 8H from encapsulation to the cracks led to a smooth layer on the surface and increased homogeneity and uniformity of coating compared to BTA and cerium as an inhibitor. However, it is noteworthy that repair defects and micro cracks by releasing inhibitors[7,8] increase the homogeneity and reduce the surface roughness.

It can be supposed that during the formation of the defects and cracks in the coating, diffusion of the inhibitors occurs and there is possibly a chemical reaction at the surface of defects to heal them. It is noticeable that high concentrations of releasing of inhibitor, especially for organic inhibitors such as 8H and BTA, reduce the strength of the network sol–gel coating and creates delamination and osmotic pressure coating and defect in the network of ceramic films.[10,11] However, organic self-healing agents due to better reaction with titanium alkoxide, help organic materials by providing a very homogeneous dispersion in the coating.

The coated samples and bare substrate were exposed to fog of 3.5 wt.% NaCl solutions under salt spray test up to 500 h and the results are summarized in Table 2.

According to Table 2, the titania-BTA nanostructured coating delivered a better protection to the substrate than the others. The performance of titania coating including cerium and 8H were almost completely tarnished with lots of pits, salt deposits and red spots. The scribed samples were seriously corroded along the scribes, which is comparable to the metal (Bare substrate) directly exposed in corrosive solution without any protection.

On the other hand, titania-BTA coating exhibits only surface discoloration after 480 h of salt spray test. It is noticed that the corrosion process occurs in three stages: first, initiation of small pits and red spot, followed by growth and spreading of deeper pits, and red area and finally the whole surface is more or less corroded with very large localized holes on the surface.[9,27] However, this result also verifies the improved corrosion resistance of BTA in aggressive Cl ion environment for long-term exposure.

Table 2. Summarized data of salt spray test at temperature of 37°C up to 500 h.

| Samples | | Exposure time (h) | | | | | | | | | | | | | | |
|---|---|---|---|---|---|---|---|---|---|---|---|---|---|---|---|---|
| | | 24 | 48 | 72 | 96 | 120 | 144 | 168 | 192 | 216 | 240 | 268 | 292 | 368 | 416 | 480 |
| SS 304 | Usual | | | | 1, 2 | 5 | | | | | | | | | | |
| | Scribed | 1,2 | 5 | | | | | | | | | | | | | |
| Titania | Usual | | | | | | | 1,2 | 3,4 | 5 | | | | | | |
| | Scribbed | | 1,2 | 5 | | | | | | | | | | | | |
| Titania-cerium | Usual | | | | | | | | 1,2 | 3,4 | 5 | | | | | |
| | Scribbed | | 1,2 | 5 | | | | | | | | | | | | |
| Titania-8H | Usual | | | | | | | | | | 1,2 | 3.4 | 5 | | | |
| | Scribbed | | 1.2 | 5 | | | | | | | | | | | | |
| Titania-BTA | Usual | | | | | | | | | | | | 1,2 | 1,2 | 3,4 | 5 |
| | Scribbed | | 1,2 | 5 | | | | | | | | | | | | |

*Note*: (1) Red spot, (2) Small pits, (3) Discoloration, (4) Rust, (5) Fail.

EIS is performed on the titania nanostructured coatings doped with the three different healing agents, $Ce(NO_3)_3$, BTA, and 8H after immersion for 1, 24, 72, and 96 h in 3.5% NaCl solution as shown in Fig. 4. The polarization resistance obtained from the diameters of the semicircles of the Nyquist plots is related to the corrosion resistance and barrier performance of the coatings. The Nyquist plots of the coated samples exhibit two or three semicircles. The first semicircles at high frequencies is associated with the barrier properties of the sol–gel coatings. The second and third semicircles at middle and low

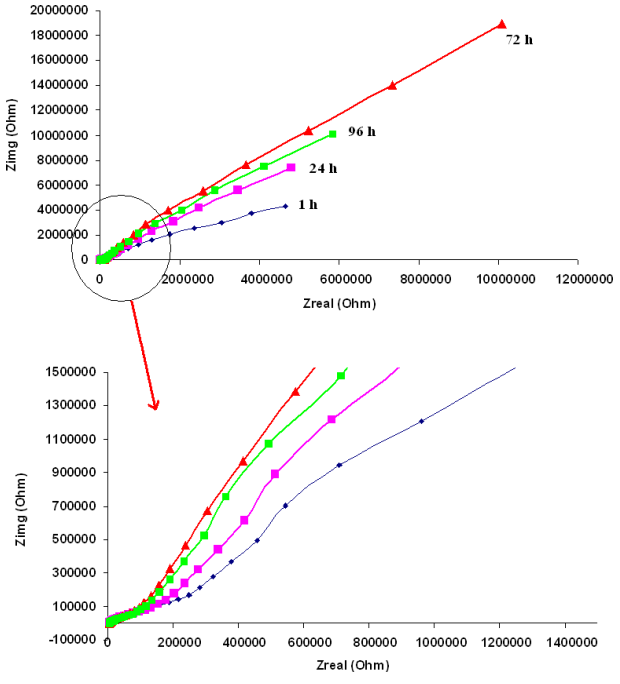


(a)

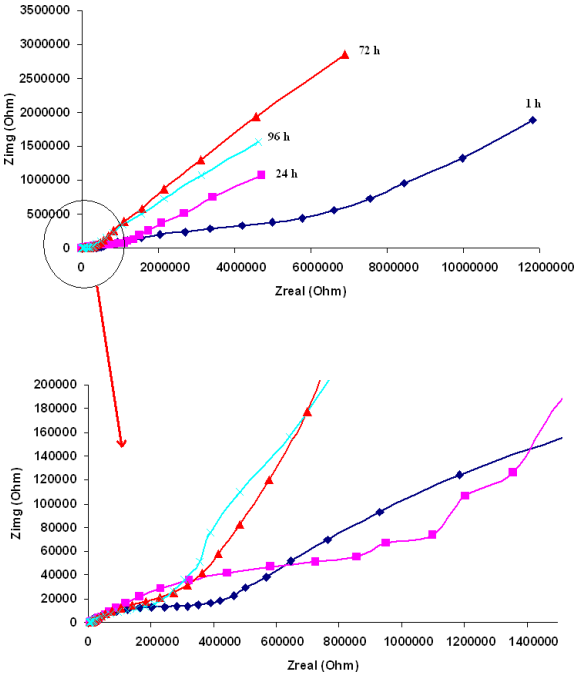


(b)

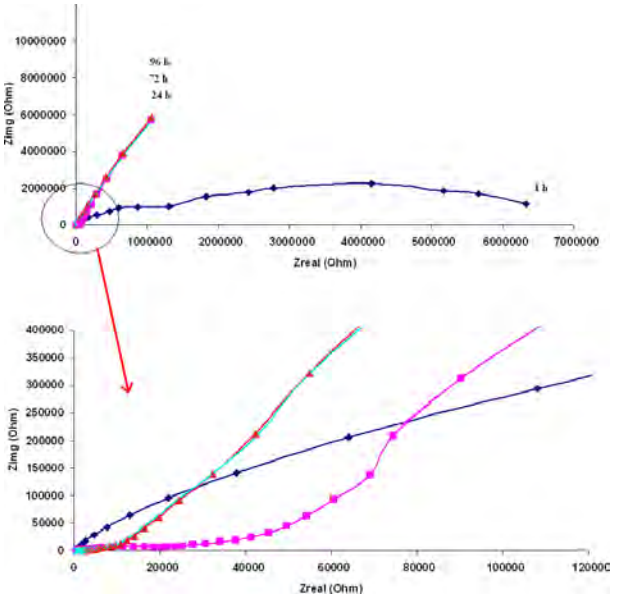


(c)

Fig. 4. EIS plots of self-healing coatings containing three different healing agents: (a) Ce, (b) 8H and (c) BTA.

frequencies depend on reduction of mass transport in the solid phase due to commencement of the healing reaction by releasing inhibitors to defects and growth of the layer, and also the charge transfer resistance of the corrosion process. The corrosion resistance of the titania coating with three different healing agents is enhanced by increasing the immersion time in 3.5% NaCl solution. The Nyquist plots demonstrate that the activation time of the coating containing 8H as an organic healing agent is enhanced when compared to other coatings including cerium and BTA. Cerium as an inorganic healing agent is second and BTA is third and maximum. Over the course of immersion, the barrier performance of the coatings changes and reduction of the impedance observed from the coatings containing Ce and 8H discloses deterioration of the protection system after immersion for 96 h in the 3.5% NaCl solution.

According to Figs. 4(a)–4(c), absorption process at the electrode surface produces the arc below the horizontal axis, which some researchers have attributed to the reactants absorbed. Actually after 1 h immersion into 3.5% NaCl solution, chloride ions with high mobility can penetrate into the holes of coating and these rings at low frequency reflect the absorption reaction on the electrode surface, the initial reactants are attracted to the surface when the metal coating is in corrosive environments. Therefore, increasing the immersion time to 72 h causes the cracks of coating to be filled by corrosion products, as a result of the reaction between the solution and the coating, to prevent the transfer times to the metal surface. On the other hand, results show the system under the control of the reactants or reaction products from the surface of the metal is dissolved. This often occurs when a species within a film is released to the electrode surface, this situation arises when the covered electrode reaction product, species or a film coating solution is absorbed.[9,27] However, after 96 h of immersion time, the concentration of chloride ions is high and causes an increase in defects, micro cracks, hole on the surface of hybrid titania nanostructured coating containing Ce and 8H by destruction of coating, and also hybrid titania nanostructured coating containing BTA, BTA is released from coating to improve the resistance of passive film, which is created on the surface.

In Fig. 4, increasing diameter of semicircle with shifting time immersion from 1 to 72 h indicates increased polarization resistance and corrosion resistance. Over time, more inhibitor molecules have been absorbed on the surface and therefore more corrosion sites are blocked. Especially, increased resistance to corrosion titania-BTA coating for 96 h immersion can be seen with adsorption inhibitors on metal surface. Inhibitory effect is dependent on two steps: first, reach the inhibitor interface metal-solution and then inhibit the absorption inhibitor on the metal surface. Replacement of organic molecules, especially BTA, at the interface instead of water molecules results in most of them being absorbed on the surface of metals. After absorption inhibitor molecules on the surface of metals, this molecules blocked the location of the active corrosion. Absorption inhibitor molecules mainly depend on some physical properties such as chemical functional groups of the molecule inhibitors, inhibitors of space, the density of electrons in electron donor atoms, and the electric charge on the surface of the metal. According to Fig. 4, the increasing polarization resistance over 72 h of immersion shows that the process of inhibitory molecules adsorbed on S.S 304 surface used during immersion time were not complete and the thermodynamic equilibrium between molecules adsorbed and molecules in solution was not achieved. Actually, the inhibitor molecules, such as cerium and 8H, also tend toward absorption of the surface and the release is not complete. However, the release of BTA constitutes a thin layer of absorption on the surface of damaged metal to prevent the influence of corrosive species. Within 48 h, almost all inhibitors were absorbed on the surface and after 72 h as shown in the diagrams at the end of a line graph, the film on the metal surface is covered and the system under control of diffusion. But after 96 h, the coating containing cerium and 8H will greatly reduce charge transfer resistance. In fact, these inhibitors, in addition to the weak corrosion inhibiting properties, can cause localized corrosion and corrosion is severed. It is noticeable that corrosion behavior of titania-BTA nanostructured coating and charge transfer resistance increased at 96 h immersion due to uptake of inhibitors on the surface.

However, when sufficient amount of inhibitors such as cerium, 8H and BTA, is released in the initial time (1 h), the holes and cracks are filled, and the film in the metal/coating interface is produced and finally leads to improved corrosion resistance. But after 72 h due to the diffusion of chloride ion and defects on the

surface, corrosion resistance of the coatings containing cerium and 8H is reduced.

On the other hand, self-healing coatings containing inhibitors improve the resistance to localized corrosion due to the formation of the protective layer which acts as a obstruction to prevent the oxygen diffusion to the metal surface, but the layer formed is relatively slim and can be destroyed by diffusion of corrosive ions and the time required for the destruction of the protective layer is increased for coating containing BTA.

An equivalent electrical circuit was proposed to explain the experimental impedance spectra. The equivalent circuit represented in Fig. 5 allows obtaining an excellent agreement between experimental and simulated impedance plots. All the fitting values for titania-based nanostructured coatings are presented in Table 3. $R_s$ is the solution resistance, $R_{\text{coat}}$ and $\text{CPE}_{\text{coat}}$ are the resistance and capacitance of the titania coating containing inhibitors such as cerium, 8H and BTA. It is mentioned that penetration of active chloride ions in the coating leads to the corrosion process, in which coatings are accompanied by appearance of a new time constant in the low frequency region, where $R_{\text{pol}}$ charge transfer resistance and $C$ double layer capacitance are added. Moreover, formation of the protective layer which acts as an obstruction to prevent the oxygen diffusion to the metal surface is presented by $\text{CPE}_{\text{oxide}}$ and $R_{\text{oxide}}$.

According to Fig. 5 and Table 3, two time constants can be considered for immersion times higher than 1 h. The time constant which slightly appears at high frequencies is related to the titania coating containing inhibitors and the one at lower frequency range to the barrier layer, which takes into account that when defects and corroded area of coating are exposed to the inhibitor, which is released from coating to defects, it is initially filled by the reaction of the inhibitor, afterwards, a progressive self-healing process occurs throughout the defects depth due to the reaction of the inhibitor with environment and its precipitation as corrosion products resulting in improvement of corrosion resistance (Fig. 5(b)). However, the barrier layer of titania coatings containing cerium and 8H after 96 h were destroyed and $C_{\text{dl}}$ and $R_{\text{corr}}$ was presented (Fig. 5(a)).

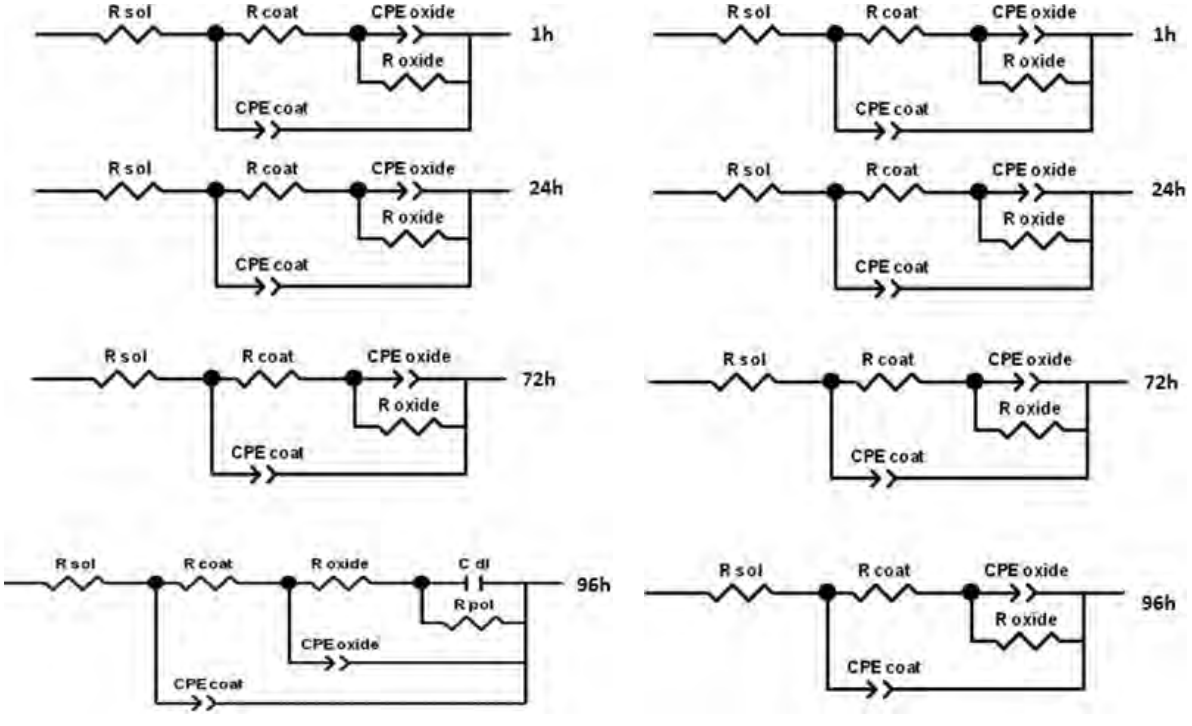


Fig. 5. Impedance spectrum modeled (simulated) electric circuit (a) titania nanostructured coating containing Ce and 8H, and (b) titania nanostructured coating containing BTA.

Table 3. EIS simulation results of the various hybrid nanostructure titania coatings with three different inhibitors, such as Cerium, BTA and 8H, in 3.5% NaCl solution.

| Sample | Immersion time (h) | $R_s$ ($\Omega \cdot cm^2$) | $R_{pore}$ ($\Omega \cdot cm^2$) | $CPE_{coat}$ ($\mu F$) | $n_{coat}$ | $R_{oxide}$ ($\Omega \cdot cm^2$) | $CPE_{oxide}$ ($\mu F$) | $n_{oxide}$ | $R_{pol}$ ($\Omega \cdot cm^2$) | $C_{dl}$ ($\mu F$) | $n_{dl}$ |
|---|---|---|---|---|---|---|---|---|---|---|---|
| Titania coating | 1 | 73 | 863 | 13.8 | 0.85 | — | — | — | 351 | 6.1 | 0.61 |
| | 24 | 79 | 819 | 12.6 | 0.85 | — | — | — | 412 | 5.9 | 0.45 |
| | 72 | 88 | 817 | 10.3 | 0.79 | — | — | — | 443 | 5.2 | 0.42 |
| | 96 | 75 | 635 | 8.4 | 0.73 | — | — | — | 334 | 6.6 | 0.39 |
| Titania-cerium coating | 1 | 79 | 351 | 5.9 | 0.72 | 814 | 4.2 | 0.78 | 638 | 5.1 | 0.64 |
| | 24 | 81 | 328 | 3.8 | 0.61 | 1126 | 2.9 | 0.73 | 610 | 5.7 | 0.58 |
| | 72 | 75 | 654 | 8.7 | 0.73 | 1809 | 1.7 | 0.69 | 851 | 3.9 | 0.48 |
| | 96 | 74 | 379 | 4.8 | 0.67 | 1267 | 3.1 | 0.71 | 794 | 4.2 | 0.49 |
| Titania-*Benzo* coating | 1 | 98 | 156 | 2.8 | 0.87 | 659 | 2.8 | 0.79 | — | — | — |
| | 24 | 102 | 52 | 9.3 | 0.78 | 1267 | 2.7 | 0.78 | — | — | — |
| | 72 | 78 | 48 | 12.7 | 0.85 | 1326 | 3.4 | 0.81 | — | — | — |
| | 96 | 81 | 48 | 10.1 | 0.76 | 1476 | 3.1 | 0.68 | — | — | — |
| Titania-8H coating | 1 | 83 | 431 | 6.8 | 0.72 | 1714 | 1.2 | 0.93 | 548 | 5.4 | 0.63 |
| | 24 | 74 | 127 | 3.3 | 0.69 | 938 | 1.1 | 0.95 | 709 | 4.7 | 0.47 |
| | 72 | 71 | 418 | 6.7 | 0.81 | 1942 | 1.6 | 0.92 | 834 | 4.1 | 0.51 |
| | 96 | 79 | 346 | 4.1 | 0.73 | 1128 | 2.1 | 0.87 | 781 | 4.6 | 0.49 |

The resistance and capacitance of the titania coating depend on the type of inhibitor, its crack ability and amount of absorbed water. In fact, water uptake into the coating and penetration of active chloride ions cause its partial destruction. It is mentioned that corrosion factors penetrating the titania coating through cracks and coating were destroyed locally. The presence of inhibitors improves the corrosion resistance of titania nanostructured coating, leading to the formation of a significant amount of corrosion product by releasing the inhibitor to defects. As a result, the corrosion resistance is considerably enhanced via titania BTA nanostructured coating. Indeed, with the addition of organic inhibitor, BTA, the healing of defects occurs than other inhibitors.

Figure 6 presents the potentiodynamic results obtained from the coated samples in 3.5% NaCl solution and corrosion parameters, such as passivity current density ($i_{passive}$) corrosion potential ($E_{corr}$), corrosion current density ($i_{corr}$), anodic and cathodic Tafel slopes ($\beta a$, $\beta c$), passive potential range ($\Delta E_{Passive}$), polarization resistance ($R$p), corrosion rate (CR) and protection efficiency which were determined from polarization curves by Tafel extrapolation method and summarized in Table 4. The application of Tafel's law assumes that the interface is under kinetic control in spite of the existence of a protection layer.[21]

Polarization resistance was derived from Stern–Geary equation,[28] as follows:

$$R_P = \frac{\beta a.\beta c}{2.3 i_{corr}(\beta a + \beta c)}. \quad (2)$$

The protection efficiency (%) was calculated according to Eq. (3):

$$\text{Protection efficiency } (\%) = \frac{i_{corr} - i_{passive}}{i_{Corr}} \times 100, \quad (3)$$

where $i_{corr}$ and $i_{passive}$ are the corrosion current densities of titania nanostructured coating and coatings including inhibitors, respectively. It is mentioned that the passivity current density gives an idea of the rate of corrosion as in Eq. (3) instead of corrosion current density of self-healing coatings. The open circuit potentials of the self-healing coating containing Ce, 8H, and BTA in 3.5% NaCl are −339, −367 and −241 mV vs SCE, respectively. The corrosion potentials of the coatings containing BTA increase to positive values. Both the anodic and cathodic branches of the coated samples shift to smaller currents, i.e. lower rates of the metal corrosion. According to results, titania nanostructured coatings containing inhibitors improve the anticorrosive properties of coating and decrease the corrosion current density compared to other coatings and shift the

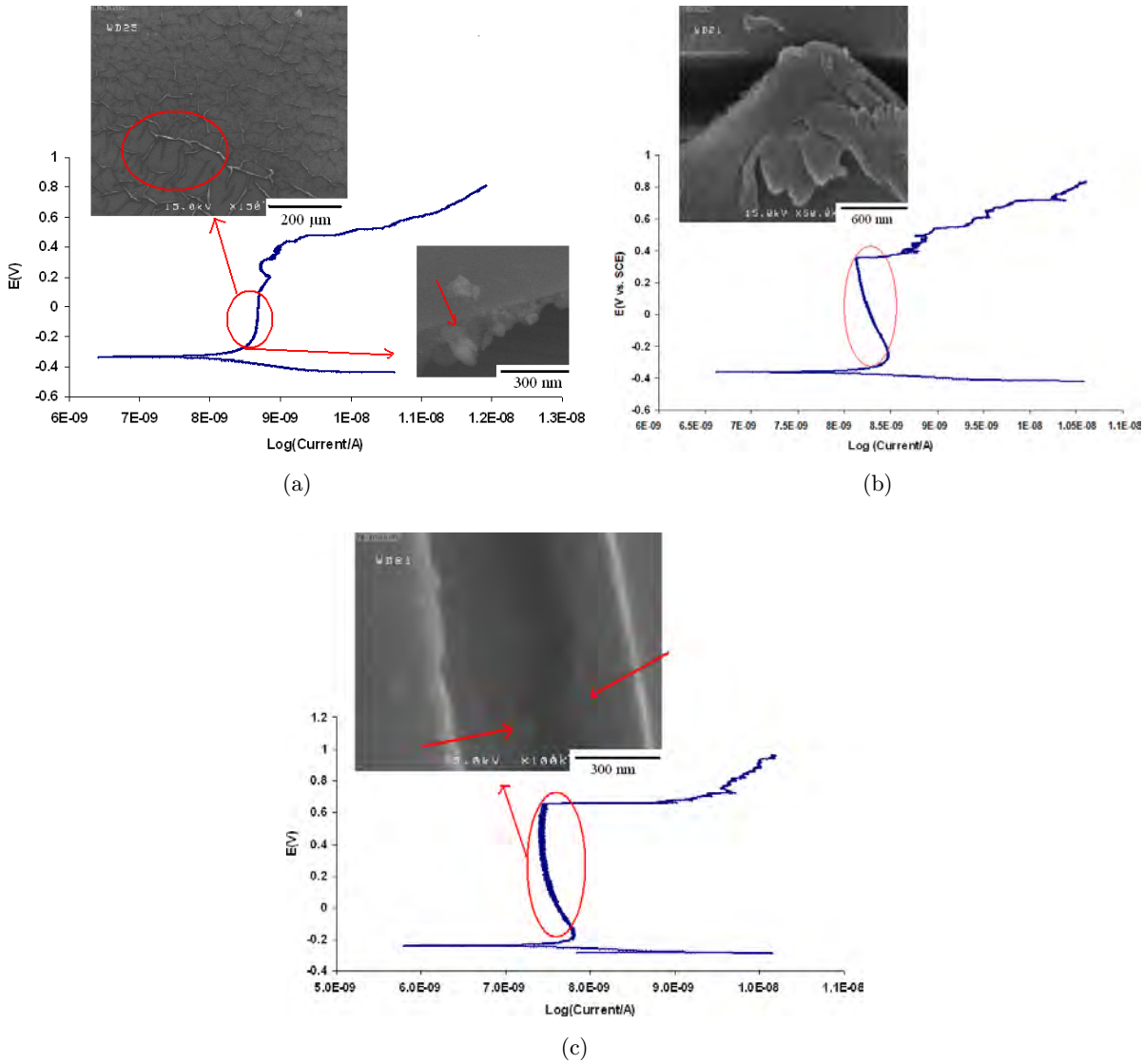


Fig. 6. Potentiodynamic polarization of self-healing coatings containing three different healing agents: (a) Ce, (b) 8H and (c) BTA.

Table 4. Potentiodynamic results of the various hybrid nanostructure titania coatings with three different inhibitors, such as Cerium, BTA and 8H, in 3.5% NaCl solution.

| Sample | $i_{\text{Passive}}$ (A) | $E_{\text{corr}}$ (V) | $i_{\text{corr}}$ (A/cm$^2$) | $\beta_a$ (V/dec) | $\beta_c$ (V/dec) | $\Delta E_{\text{Passive}}$(v) | $R_p$ ($\Omega \cdot$cm$^2$) | CR (mm/y) | Protection efficiency (%) |
|---|---|---|---|---|---|---|---|---|---|
| Titania coating | — | −0.546 | 7.73E-06 | 0.123 | 0.213 | — | 4.38E+03 | 13.06E-02 | |
| Titania-cerium coating | 8.6E-09 | −0.339 | 7.9E-09 | 0.026 | 0.02 | 0.395 | 6.22E+05 | 1.45E-04 | 99.88 |
| Titania-8H coating | 8.31E-09 | −0.367 | 8.06E-09 | 0.063 | 0.01 | 0.599 | 4.69E+05 | 1.40E-04 | 99.89 |
| Titania-*Benzo* coating | 7.5E-09 | −0.241 | 7.06E-09 | 0.019 | 0.014 | 0.825 | 5.01E+05 | 1.27E-04 | 99.5791 |

corrosion potential towards more positive value, which indicates a passivating effect of the coating. The passivation region on the coated sample, especially the self-healing coating containing BTA, is stable from −198 mV to 627 mV ($\Delta E_{\text{Passive}}$ value is about 825 mV), and also the passivation current density is around $10^{-8}$ A/cm$^2$. Indeed, this coating shows low passive current densities with a wide passive potential range when compared to other coatings. The higher corrosion resistance of the BTA containing coating can be related to the quick formation of a noble and protective passive film.

In the following, for understanding barrier performance and corrosion protection of self-healing coatings containing inhibitors, passivity behavior should be analyzed further. The passivity loss leading to localized corrosion or pitting in passive metals results from a variety of different mechanisms, such as the penetration mechanism, the film breaking mechanism and the adsorption mechanism.[29] These mechanisms involve breaks (e.g. blistering, accumulation of vacancies, electrostriction stress, microcapillary formation and the crack-heal mechanism) within the film, and the transfer of anions (aggressive ion such as $Cl^-$) through the oxide film to the metal surface and the occurrence of the breakdown of the oxide layer once they reach the underlying bare metal. Actually, adsorption of aggressive ions on the protective oxide film is considered as the first step towards the passivity breakdown. The next step consists of the transport of $Cl^-$ ions through the oxide film by means of oxygen vacancies, followed by a local dissolution of substrate at the metal–oxide interface. Finally, adsorption of aggressive anions reduced the surface tension of the passive film such that cracks would arise, allowing anions to reach the metal surface. Especially for stainless steel, pits occur as a result of mechanical rupture of the passive film brought about by salt film formation underneath the film. However, according to Table 1, healing agents can improve surface properties by decreasing roughness of surface and healing defects and lead to decreased adsorption and transport of aggressive ions on the coatings including organic inhibitor, i.e. 8H and BTA. The healing was considered to occur by releasing the inhibitor and migration of oxygen anions towards the defects. Among inhibitors, BTA, which presents a wide passivity range, plays an important role to enhance the barrier performance of coatings and decreased diffusion rate of $Cl^-$.

## 4. Conclusion

Hybrid self-healing coatings are prepared by hydrolysis of organically modified silicon alkoxide (GPTMS) condensed with a metallic alkoxide (Ti) and healing agents including Ce, BTA, and 8H. Formation of a nanoporous $TiO_2$ structure enhances the homogeneous distribution and loading capacity of the healing agents in the coatings. The presence of a porous $TiO_2$ intermediate layer provides good adhesion between the sol–gel coatings and 304 stainless steel substrates. The self-healing coatings containing BTA yield better protection than those containing Ce and 8H. The self-healing properties of the coating containing 8H are enhanced when compared to other coatings including cerium and BTA, followed by the Ce incorporated coating and the BTA gained the minimum.

## Acknowledgments

The authors would like to express their thanks to Iranian Nanotechnology Initiative Council. The work was financially supported by City University of Hong Kong Applied Research Grants 9667066 and Malayer University Applied Research Grants.

## References

1. E. Ghali, *Uhlig's Corrosion Handbook*, ed. R. W. Revie (John Wiley & Sons, New York, 2000).
2. J. E. Gray and B. Luan, *J. Alloys Compd.* **336** (2002) 88–113.
3. A. S. Hamdy, I. Doench and H. Möhwald, *Prog. Org. Coat.* **72** (2011) 387–393.
4. M. Samadzadeha, S. Hatami Boura, M. Peikari, S. M. Kasiriha and A. Ashrafi, *Prog. Org. Coat.* **68** (2010) 159–164.
5. V. K. Thakur and M. R. Kessler, *Polymer* **69** (2015) 369–383.
6. M. Abdolah Zadeh, S. van der Zwaag and S. J. García, *Surf. Coat. Technol.* **303** (2016) 396–405.
7. M. Wang, M. Liu and J. Fu, *J. Mater. Chem. A* **3** (2015) 6423–6431.
8. M. L. Zheludkevich, D. G. Shchukin, K. A. Yasakau, H. Möhwald and M. G. S. Ferreira, *Chem. Mater.* **19** (2007) 402–411.
9. M. Huang and J. Yang, *Prog. Org. Coat.* **77** (2014) 168–175.
10. V. Sauvant-Moynot, S. Gonzalez and J. Kittel, *Prog. Org. Coat.* **63** (2008) 307–315.
11. S. V. Lamaka, M. L. Zheludkevich, K. A. Yasakau, R. Serra, S. K. Poznyak and M. G. S. Ferreira, *Prog. Org. Coat.* **58** (2007) 127–135.

12. A. F. Galio, S. V. Lamaka, M. L. Zheludkevich, L. F. P. Dick, I. L. Müller and M. G. S. Ferreira, *Surf. Coat. Technol.* **204** (2010) 1479–1486.
13. M. L. Zheludkevich, R. Serra, M. F. Montemor, I. M. Miranda Salvado and M. G. S. Ferreira, *Surf. Coat. Technol.* **200** (2006) 3084–3094.
14. Y.-H. Han, A. Taylor and K. M. Knowles, *Surf. Coat. Technol.* **202** (2008) 1859–1868.
15. X. Zhong, Q. Li, J. Hu and Y. Luorr, *Corros. Sci.* **50** (2008) 2304.
16. D. G. Shchukin, M. L. Zheludkevich, K. Yasakau, S. Lamaka, M. G. S. Ferreira and H. Möwald, *Adv. Mater.* **18** (2006) 1672.
17. D. Wang and G. P. Bierwagen, *Prog. Org. Coat.* **64** (2009) 327–338.
18. A. Abou-Elazm, R. Abdel-Karim, I. Elmahallawi and R. Rashad, *Corros. Sci.* **51** (2009) 203–208.
19. X. Fang, K. Zhang, H. Guo, W. Wang and B. Zhou, *Mater. Sci. Eng. A* **487** (2008) 7–13.
20. M. Aparicio, A. Jitianu, G. Rodriguez, A. Degnah, K. Al-Marzoki, L. C. Klein and J. Mosa, *Electrochim. Acta* **202** (2016) 325–332.
21. L. Curkovic, H. O. Curkovic, S. Salopek, M. M. Renjo and S. Šegota, *Corros. Sci.* **77** (2013) 176–184.
22. A. Marsal, F. Ansart, V. Turq, J. P. Bonino, J. M. Sobrino, Y. M. Chen and J. Garcia, *Surf. Coat. Technol.* **237** (2013) 234–240.
23. R. Subasri, R. Malathi, A. Jyothirmayi and N. Y. Hebalkar, *Ceram. Int.* **38** (2012) 5731–5740.
24. N. C. Rosero-Navarroa, L. Paussa, F. Andreatta, Y. Castro, A. Durán, M. Aparicio and L. Fedrizzi, *Prog. Org. Coat.* **69** (2010) 167–174.
25. K. A. Yasakau, M. L. Zheludkevich, O. V. Karavai and M. G. S. Ferreir, *Prog. Org. Coat.* **63** (2008) 352–361.
26. N. C. Rosero-Navarro, S. A. Pellice, A. Durań and M. Aparicio, *Corros. Sci.* **50** (2008) 1283–1291.
27. S. Manivannan, S. K. Gopalakrishnan, S. P. Kumaresh Babu and S. Sundarrajan, *Alexandria Eng. J.* **55** (2016) 663–671.
28. R. B. Figueira, C. J. R. Silva and E. V. Pereira, *J. Electrochem. Soc.* **162** (2015) C666–C676.
29. J. Soltis, *Corros. Sci.* **90** (2015) 5–22.